M&MS

DESIGNING A SIMPLE RADIOMETRIC SYSTEM TO PREDICT VOID FRACTION PERCENTAGE INDEPENDENT OF FLOW PATTERN USING RADIAL BASIS FUNCTION

Gholam H. Roshani[1], Ehsan Nazemi[2], Farzin Shama[3], Mohammad A. Imani[4], Salar Mohammadi[5]

1) *Kermanshah University of Technology, Electrical Engineering Department, Kermanshah, Iran* (*hosseinroshani@yahoo.com*)
2) *Nuclear Science and Technology Research Institute, Tehran, Iran* (✉ *enazemi@aeoi.org.ir,* +98 91 3200 7423)
3) *Islamic Azad University, Department of Electrical Engineering, Kermanshah Branch, Kermanshah, Iran* (*f.shama@aut.ac.ir*)
4) *Kermanshah University of Medical Sciences, Medical Biology Research Centre, Kermanshah, Iran* (*imani.mohammadamin@stu.razi.ac.ir*)
5) *Islamic Azad University, Young Researchers and Elite Club, Kermanshah Branch, Kermanshah, Iran* (*mohamady.salar@yahoo.com*)

Abstract

The void fraction is one of the most important parameters characterizing a multiphase flow. The prediction of the performance of any system operating with more than single phase relies on our knowledge and ability to measure the void fraction. In this work, a validated simulation study was performed in order to predict the void fraction independent of the flow pattern in gas-liquid two-phase flows using a gamma ray ^{60}Co source and just one scintillation detector with the help of an *artificial neural network* (ANN) model of *radial basis function* (RBF). Three used inputs of ANN include a registered count under Compton continuum and counts under full energy peaks of 1173 and 1333 keV. The output is a void fraction percentage. Applying this methodology, the percentage of void fraction independent of the flow pattern of a gas-liquid two-phase flow was estimated with a mean relative error less than 1.17%. Although the error obtained in this study is almost close to those obtained in other similar works, only one detector was used, while in the previous studies at least two detectors were employed. Advantages of using fewer detectors are: cost reduction and system simplification.

Keywords: two-phase flow, gamma ray attenuation, scintillation detector, void fraction, artificial neural network.

1. Introduction

A great demand in the world for oil and gas has been the main motivation for petroleum companies to continually look for approaches to enhance oil and gas production techniques. The objectives have included making marginal fields more cost-effective, establishing production fa-

www.czasopisma.pan.pl PAN www.journals.pan.pl
G.H. Roshani, E. Nazemi, et al.: DESIGNING A SIMPLE RADIOMETRIC SYSTEM TO PREDICT...
POLSKA AKADEMIA NAUK

cilities in difficult physical environments, reducing the development cost and improving the energy efficiency of new fields. The multiphase flow-meters play an important role in the mentioned fields and every try which leads to improvement in this technique is of great importance.

The void fraction is a key parameter characterizing a gas-liquid two-phase flow. To date, various methods such as volumetric, electrical, optical, ultrasonic and nuclear radiation techniques have been introduced for measuring the void fraction. By comparing all the measurement methods, it can be seen that the gamma ray attenuation method has been widely used because of its advantages, such as its non-intrusiveness and greater reliability. However, this method has some disadvantages, such as physical health problems and safety.

In recent years, a large number of researchers have investigated the use of gamma ray attenuation in determination of the void fraction in gas-liquid two-phase flows. Abro *et al.* performed a simulation study in order to determine the type of flow regime and the void fraction in gas-liquid two-phase flows using EGS4 software package and ANN. Their simulation geometry included three detectors and one ^{241}Am source. Using this geometry, they could distinguish all the three ideal flow regimes (annular, stratified and homogenous) and also determine the void fraction with an error of less than 3% [1]. Roshani *et al.* used validated simulations and an ANN in order to recognize the type of flow regime and then estimate the void fraction in gas-liquid two-phase flows [2]. Their simulation configuration included a ^{137}Cs source and two scintillation NaI detectors. They used the total count in the scattering detector, the full energy peak and photon counts of Compton edge in the transmission detector as the three inputs of the ANN. By using this methodology, they could correctly recognize all three flow regimes – stratified, homogenous and annular – and also predict the void fraction of each phase in a range of 5–95% with an error of less than 1.1%. Adineh et al. carried out an experimental study of measuring the void fraction for a modelled two-phase flow inside a vertical pipe by using gamma rays [3]. They modelled three types of typical flow regimes, *i.e.* homogenous, stratified and annular ones, in a vertical pipe by using polyethylene phantoms. Their experimental setup consisted of a ^{137}Cs source and two scintillation NaI detectors. For three modelled flow regimes, all transmitted and scattered gamma rays in all directions were measured by setting the gamma ray source and the detector around the pipe. They also used the MCNP code to provide an appropriate correction coefficient for measuring the void fraction and to improve the accuracy and validation of experimental results. Nazemi *et al.* designed an experimental setup in order to predict the void fraction in gas-liquid two-phase flows independent of the type of flow regime [4]. They employed one radioactive source and two NaI detectors for registering the transmitted photons. The counts registered in both detectors were used as inputs of an ANN model of a *multi-layer perceptron* (MLP). Applying this methodology, the void fraction percentage was estimated with a mean relative error less than only 1.4%. More studies on radiation-based multiphase flow-meters and also application of ANN in nuclear engineering can be found in the references [5–27].

As it was mentioned, in all previous works two or more detectors were used in order to measure the void fraction in gas-liquid two-phase flows. Using fewer detectors is advantageous in industrial nuclear gauges since it offers both cost reduction and improved simplicity. In this work we used one source and one detector to determine the void fraction in gas-liquid two-phase flows independent of the type of flow regime. This geometry was proposed in our recently published work [28] for identifying the flow regime. Unfortunately, in that paper it was demonstrated that it is not possible to recognize all the flow regimes in gas-liquid two-phase flows using one detector, one radioactive source and an ANN model of MLP. In fact, in the presented paper we will demonstrate that it is possible to predict the void fraction independent of the flow pattern, although recognizing the flow regime is not possible.

2. Materials and method

2.1. Monte Carlo simulation

In this study, the *Monte Carlo N-Particle* (MCNP) code, version X, was used. MCNP is a useful tool for radiation transport, mainly in situations where physical measurements are impracticable or inconvenient. The detection configuration consists of one NaI(Tl) scintillator detector which is placed diametrically to a ^{60}Co source. For simulating the NaI(Tl) scintillator detector, the crystal itself was considered as a homogeneous cylinder. The dimensions of detector are 25.4 mm in thickness and 25.4 mm in diameter. A collimated (a cubic collimator 0.6 cm wide, 2 cm high and 10 cm long) gamma-ray point source was also simulated in order to produce a narrow beam. A Pyrex-glass pipe composed of a test section with 2.5 mm thickness and the maximum outside diameter of 100 mm, was simulated as the main pipe. The detector was placed at the distances of 10 cm and 30 cm from the centre of pipe and the source, respectively. The simulation configuration is shown in Fig. 1. It should be noted that the simulation geometry has been benchmarked with the laboratory experiments in our previous works [2, 14, 15].
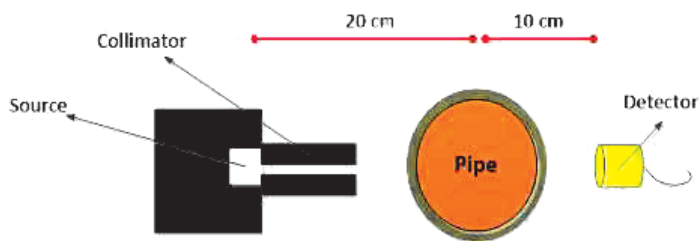
Fig. 1. The simulated geometry.

Air with a density of 0.00125 g/cm^3 was used as the air phase in all simulations. Also, gasoil with a density of 0.826 g/cm^3 and the chemical formula $C_{12}H_{23}$ was used as the liquid phase. Three flow regimes (stratified, annular and homogenous) in gas-liquid two-phase flows were simulated (more details about simulation of flow regimes can be found in [28]). These three flow regimes are the basic regimes in gas-liquid two-phase flows and other flow regimes are incorporated in these patterns. In each flow regime, void fractions with the values in a range of 5–95% and steps of 5%, were simulated in order to provide the data sets required for testing and training the ANN. In fact, 57 simulations were carried out. Three simulated flow regimes are shown in Fig. 2.
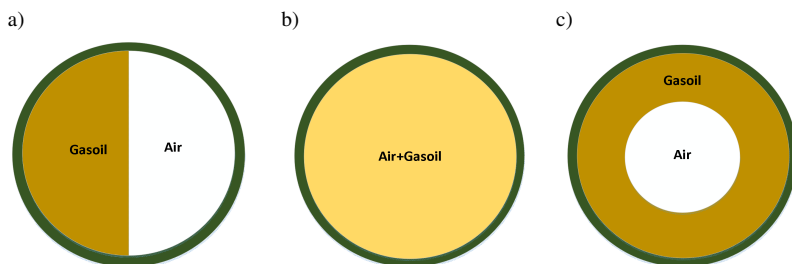
Fig. 2. Simulated two-phase flow regimes: a) Stratified; b) Homogenous; c) Annular.

www.czasopisma.pan.pl   PAN   www.journals.pan.pl
G.H. Roshani, E. Nazemi, et al.: DESIGNING A SIMPLE RADIOMETRIC SYSTEM TO PREDICT . . .
POLSKA AKADEMIA NAUK

The MCNP-X Monte Carlo computer code provides also a special data treatment suitable for gamma-ray spectrum data acquisition, which is the *Gaussian energy broadening* (GEB) (card FTn) option. It is used to fit the full energy peak shape of the gamma-ray spectrum to a Gaussian response of an experimental measurement [29]. The technique consists of using an "FT8 GEB" card in the input file of MCNP code and calculating the *full width at half maximum* (FWHM) of the full energy peak of gamma rays with different energies in the laboratory. It should be noted that the counts registered in the detector were calculated per one source particle in the MCNP-X code using Pulse Height Tally F8. The desired FWHM, which should be determined by the user-provided constants (a, b, and c), has a nonlinear response relative to energy according to the equation (1) [29]:

$$\text{FWHM} = a + b\sqrt{E + cE^2},\qquad(1)$$

where E is an incident gamma-ray energy. The units of "a", "b" and "c" parameters are MeV, MeV$^{1/2}$, and MeV^{-1}, respectively. To determine "a", "b" and "c" parameter values, one 25.4×25.4 mm scintillator NaI detector and 3 gamma emitter radioactive sources of ^{241}Am (energy 59.5 keV), ^{137}Cs (energy 662 keV) and ^{60}Co (energies 1173 and 1333 keV) including four gamma energies in a range of 59.5–1333 KeV, were used. The experimental spectra for ^{241}Am, ^{137}Cs and ^{60}Co sources are shown in Fig. 3. At first, FWHM of each photo peak was calculated in terms of number of channels which should be converted in terms of energy (MeV) by using (2):

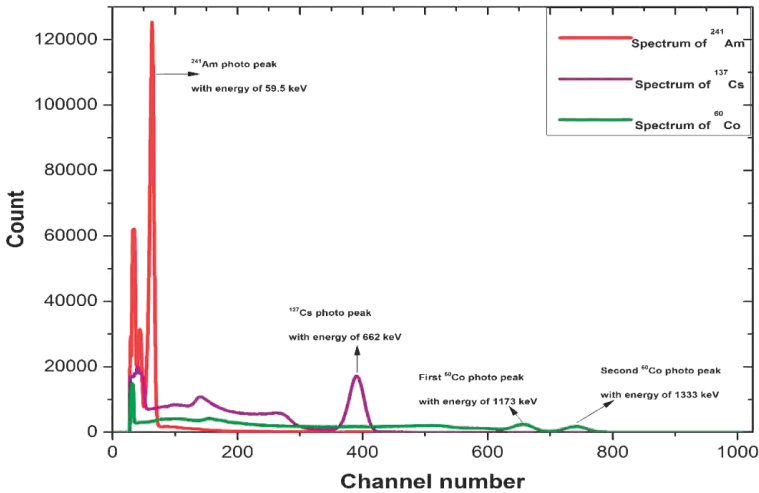$$\text{FWHM (MeV)} = \frac{\text{FWHM(channel)} \times \text{Energy of peak (MeV)}}{\text{Channel's number of peak(channel)}}.\qquad(2)$$

Fig. 3. The experimental spectra registered in the 25.4×25.4 mm scintillator NaI detector for the radioactive sources of ^{241}Am, ^{137}Cs and ^{60}Co.

FWHMs of each photo peak are shown in Table 1.

As shown in Fig. 4, after obtaining the experimental FWHM values for each photo peak, FWHM (MeV) was plotted as a function of energy of photo peaks (MeV). A non-linear fitting function was implemented for this curve in order to determine the values of "a", "b" and "c".

Table 1. Calculated full widths at half maximum (FWHMs) for photo peaks with energies of 60, 662, 1173 and 1333 keV in the 25.4 × 25.4 mm NaI detector.

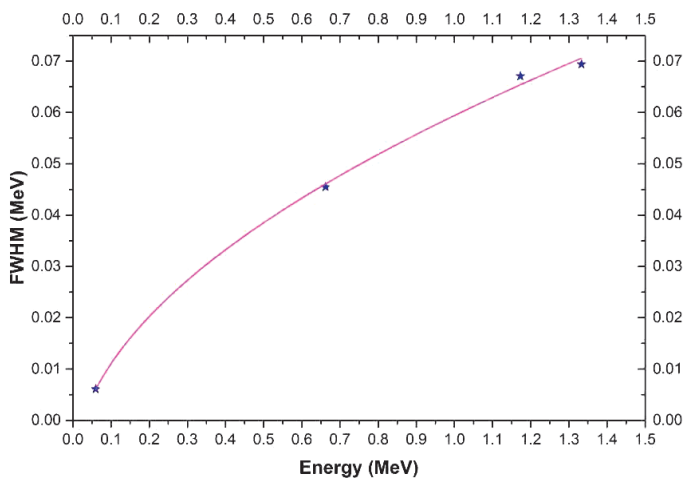| Energy of photo peak (keV)	FWHM (number of channels)	FWHM (energy with unit of MeV)
59.5	6.45	0.0061
662	26.83	0.0455
1173	37.51	0.0671
1333	38.59	0.0694

Fig. 4. Calculation of GEB card parameters using FWHM values obtained for different energies and a non-linear fitting function.

The values of "*a*", "*b*" and "*c*" parameters are shown in Table 2. They were calculated with the GEB command in the input file of MCNP code to take account of the energy resolution of the 25.4 × 25.4 mm scintillator NaI detector in the simulations.

Table 2. The values of required parameters calculated with the GEB command in the input file of MCNP codein order to take account of the energy resolution.

Parameters	Value
a (MeV)	0.0109
b (MeV$^{1/2}$)	0.0696
c (MeV^{-1})	0.0226

In each void fraction value, three features (count under Compton continuum and counts under photo peaks with energies of 1173 and 1333 keV) were extracted from the gamma-ray spectrum registered in the detector. In the case of count under Compton continuum, only Compton continuum related to gamma with energy of 1173 keV and Compton edge of 963 keV, was considered. The counts registered in the detector versus the void fraction are shown in Fig. 5 for three flow regimes: annular, homogenous and stratified.
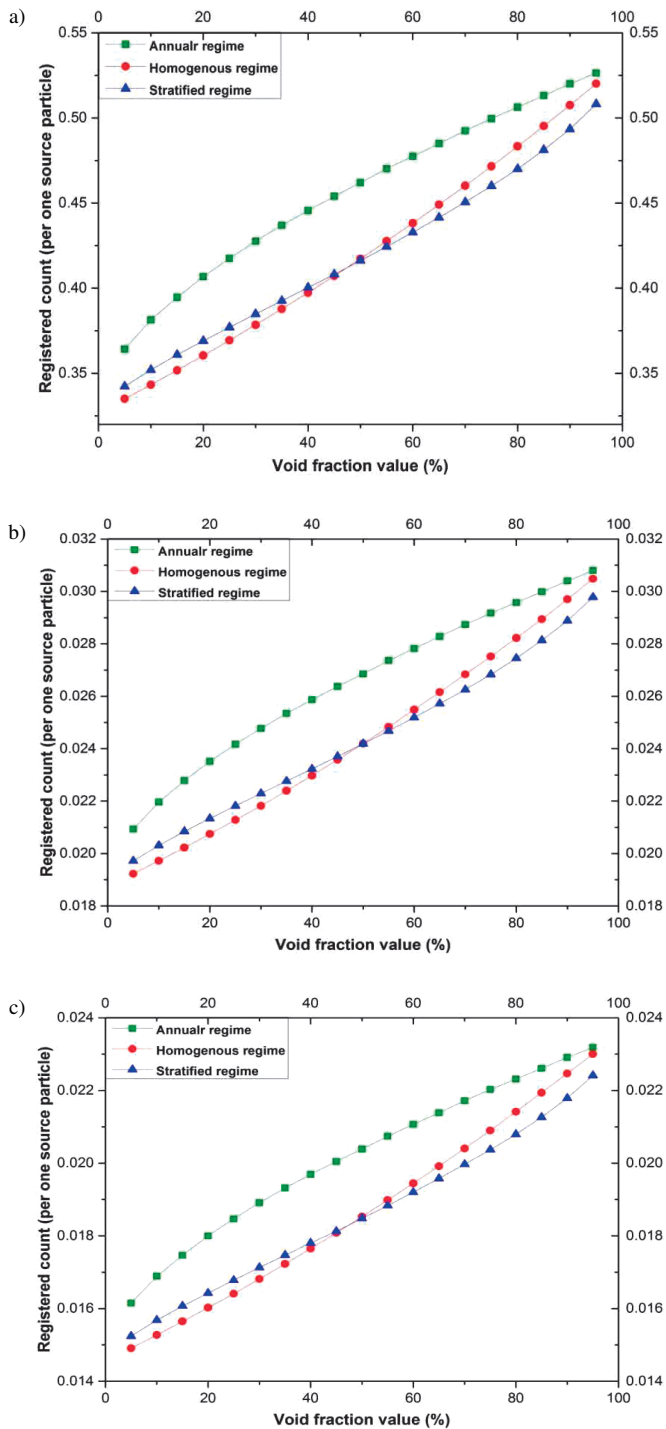
351

Fig. 5. Registered counts versus void fraction for annular, homogenous and stratified flow regimes: a) count under Compton continuum; b) count under photo peak with energy of 1173 keV; c) count under photo peak with energy of 1333 keV.

2.2. Radial basis function network

Artificial neural networks (ANNs) are applied to simulating system performance, especially in the case of simulating complex systems, while a limited volume of experimental data is available. A neural network includes many neurons as processing elements, which are connected by synaptic weights [30]. The *radial basis function* (RBF) ANNs are the feed-forward types of networks with three layers, usually with a Gaussian activation function for each neuron in the hidden layer and a linear transfer function in the output layer [31]. The numbers of neurons in the input and output layers depend on the numbers of input and output data, respectively. Simple structure, fast training process, good ability in controlling input noise, suitable generalization capability, and ability of online learning in comparison with other feed-forward ANNs are some advantages of the RBF networks [32]. The conventional structure of an RBF is shown in Fig. 6. An RBF measures the distance between the input vectors and the weight vectors and is typically considered to be a Gaussian function. Thus, the output of this network can be given by [33]:

$$Y = \sum_{j=1}^{L} W_j f_j = \sum_{j=1}^{L} W_j \exp\left(-\frac{1}{2\sigma^2}\|I - C_j\|^2\right), \tag{3}$$

where C_j is the centre vector for the jth hidden node determined by the K-means clustering method, $\|I - C_j\|$ is the Euclidean norm and σ^2 is the variance of the Gaussian function.
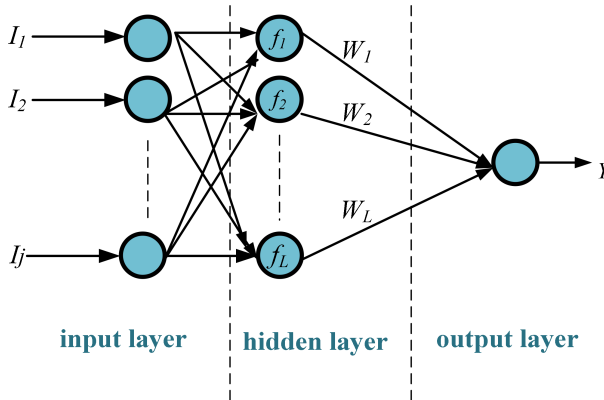

Fig. 6. The conventional structure of an RBF.

The used inputs are three features extracted from the gamma spectrum (counts under full energy peaks of 1.173 and 1.333 MeV and count under Compton continuum) for the designed RBF model, as shown in Fig. 7. The output of the architecture includes the void fraction percentage of gas. The designed architecture is shown in Fig. 8. The designed network includes only three neurons in the hidden layer. Therefore, it can be concluded that it is an optimized RBF network.

As it can be seen from Table 3, the required training-data set was created from all of three regimes and divided into two overall sets: 70% as training data and 30% as testing data. The configuration of the designed RBF network is presented in Table 4.

www.czasopisma.pan.pl PAN www.journals.pan.pl

G.H. Roshani, E. Nazemi, et al.: DESIGNING A SIMPLE RADIOMETRIC SYSTEM TO PREDICT . . .
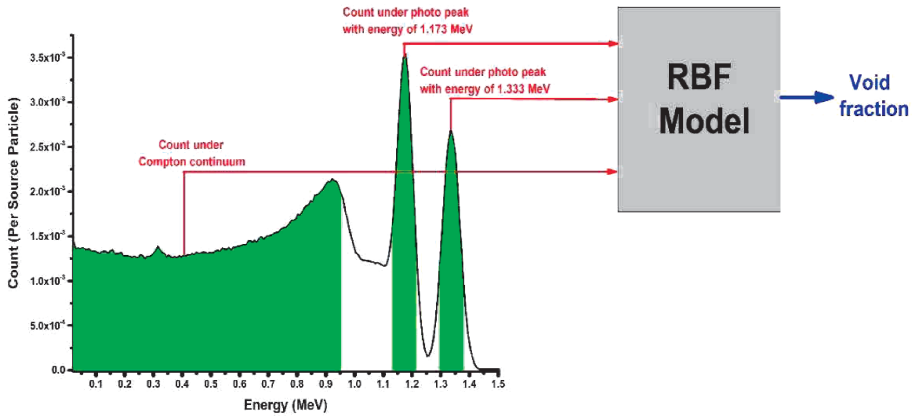

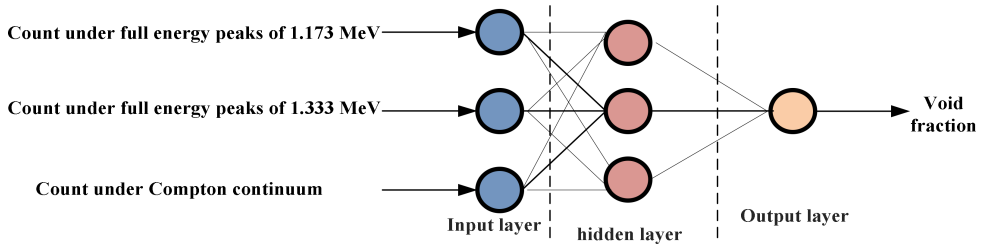Fig. 7. The inputs and output of an RBF model.

Fig. 8. The architecture of the designed RBF model.

Table 3. The training-data set created from all of three regimes.

Annular regime				Homogenous regime				Stratified regime			
void	Compton	1.17 peak	1.33 peak	void	Compton	1.17 peak	1.33 peak	void	Compton	1.17 peak	1.33 peak
5	3.64E-01	2.09E-02	1.62E-02	5	3.35E-01	1.92E-02	1.49E-02	5	3.42E-01	1.97E-02	1.52E-02
10	3.81E-01	2.20E-02	1.69E-02	10	3.43E-01	1.97E-02	1.53E-02	10	3.52E-01	2.03E-02	1.57E-02
15	3.95E-01	2.28E-02	1.75E-02	15	3.52E-01	2.02E-02	1.57E-02	15	3.61E-01	2.08E-02	1.61E-02
20	4.07E-01	2.35E-02	1.80E-02	20	3.60E-01	2.07E-02	1.60E-02	20	3.69E-01	2.13E-02	1.64E-02
25	4.18E-01	2.42E-02	1.85E-02	25	3.69E-01	2.13E-02	1.64E-02	25	3.77E-01	2.18E-02	1.68E-02
30	4.28E-01	2.48E-02	1.89E-02	30	3.78E-01	2.18E-02	1.68E-02	30	3.85E-01	2.23E-02	1.71E-02
35	4.37E-01	2.53E-02	1.93E-02	35	3.88E-01	2.24E-02	1.72E-02	35	3.93E-01	2.28E-02	1.75E-02
40	4.46E-01	2.59E-02	1.97E-02	40	3.97E-01	2.30E-02	1.77E-02	40	4.00E-01	2.32E-02	1.78E-02
45	4.54E-01	2.64E-02	2.00E-02	45	4.07E-01	2.36E-02	1.81E-02	45	4.08E-01	2.37E-02	1.81E-02
50	4.62E-01	2.69E-02	2.04E-02	50	4.17E-01	2.42E-02	1.85E-02	50	4.16E-01	2.42E-02	1.85E-02
55	4.70E-01	2.74E-02	2.07E-02	55	4.28E-01	2.48E-02	1.90E-02	55	4.24E-01	2.47E-02	1.88E-02
60	4.77E-01	2.78E-02	2.11E-02	60	4.38E-01	2.55E-02	1.94E-02	60	4.33E-01	2.52E-02	1.92E-02
65	4.85E-01	2.83E-02	2.14E-02	65	4.49E-01	2.62E-02	1.99E-02	65	4.41E-01	2.57E-02	1.96E-02
70	4.92E-01	2.87E-02	2.17E-02	70	4.60E-01	2.68E-02	2.04E-02	70	4.51E-01	2.63E-02	2.00E-02
75	5.00E-01	2.92E-02	2.20E-02	75	4.72E-01	2.75E-02	2.09E-02	75	4.60E-01	2.68E-02	2.04E-02
80	5.06E-01	2.96E-02	2.23E-02	80	4.83E-01	2.82E-02	2.14E-02	80	4.70E-01	2.75E-02	2.08E-02
85	5.13E-01	3.00E-02	2.26E-02	85	4.95E-01	2.89E-02	2.19E-02	85	4.81E-01	2.81E-02	2.13E-02
90	5.20E-01	3.04E-02	2.29E-02	90	5.07E-01	2.97E-02	2.25E-02	90	4.93E-01	2.89E-02	2.18E-02
95	5.26E-01	3.08E-02	2.32E-02	95	5.20E-01	3.05E-02	2.30E-02	95	5.08E-01	2.98E-02	2.24E-02

Table 4. The configuration of the designed RBF network.

ANN type	RBF
No. of neurons in the input layer	3
No. of neurons in the hidden layer	3
No. of neurons in the output layer	1
Spread	0.4
Target Error	0
Activation function	Gaussian

3. Results

The results predicted with the designed RBF model compared with the real results can be explained as regression diagrams for the training and testing processes. The regression diagrams for the training and testing procedures are shown in Figs. 9 and 10, respectively.
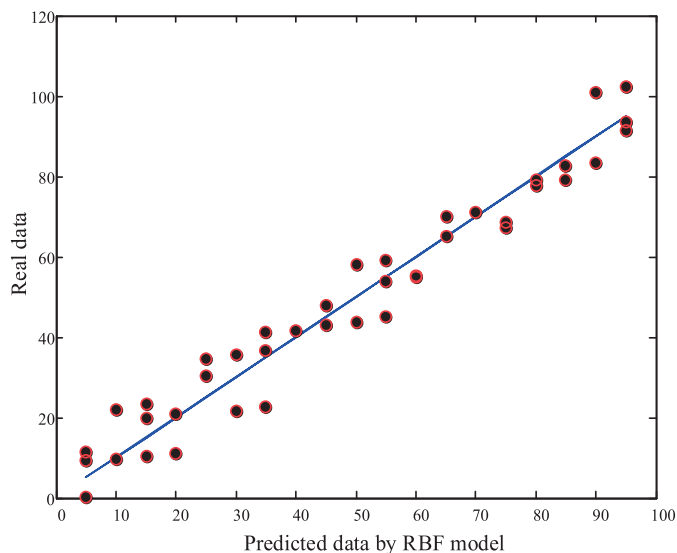

Fig. 9. Regression diagrams for the training procedure.

Table 5 shows the obtained defined errors for the designed RBF model. The defined errors contain mean absolute error percentage (MAE %), mean relative error percentage (MRE %) and *root mean square error* (RMSE), which has been calculated as [21]:

$$\text{MRE\%} = 100 \times \frac{1}{N} \sum_{i=1}^{N} \left| \frac{X_i(\text{Re}) - X_i(\text{Pr})}{X_i(\text{Re})} \right|, \tag{4}$$

$$\text{RMSE} = \left[\frac{\sum_{i=1}^{N} (X_i(\text{Re}) - X_i(\text{Pr}))^2}{N} \right]^{0.5}, \tag{5}$$
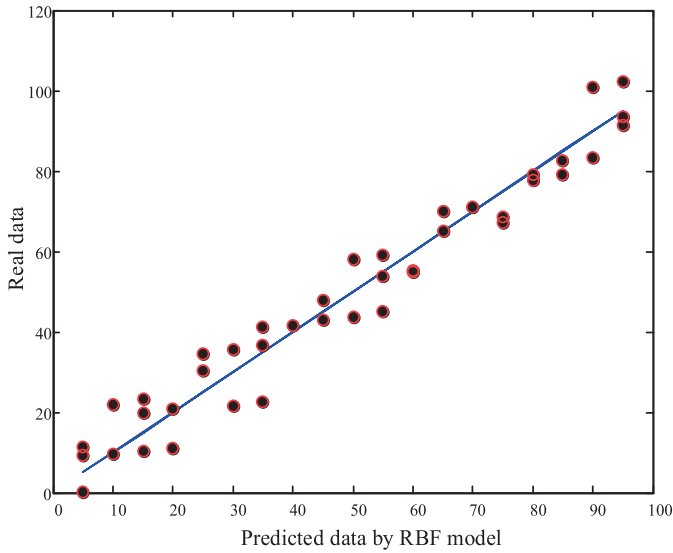
355

Fig. 10. Regression diagrams for the testing procedure.

$$\text{MAE\%} = \frac{1}{N} \sum_{i=1}^{N} |X_i(\text{Re}) - X_i(\text{Pr})|, \tag{6}$$

where N is the number of data and 'X(Re)' and 'X(Pr)' denote the real data and the RBF-predicted data, respectively. As can be seen from Table 5, the obtained errors for the test data are small, which is acceptable when considering only one detector.

Table 5. The obtained defined errors of the designed MLP network.

Defined Errors	Train	Test
MAE%	5.18	3.73
MRE%	1.17	0.37
RMSE	6.12	4.54

One of the significant advantages of the proposed RBF model is its simplicity and precision. Therefore, the designed model is a good tool of predicting the void fraction from the mentioned features with an acceptable accuracy.

4. Conclusion

In this research, a simple RBF neural network has been applied to estimate the void fraction in a gas-liquid two-phase flow. Using just one detector and predicting the void fraction independent of the flow regime's type are advantages of the presented methodology. First, with the help of MCNP code, three main flow regimes (annular, stratified and homogenous) with various void fractions were modelled. After that, in each void fraction three features from the registered spectrum of ^{60}Co were extracted. Then, the extracted features including counts under full energy peaks of 1.173 and 1.333 MeV and count under Compton continuum were used as inputs of the

RBF network and the void fraction was considered as the output. Finally, the RBF model could predict the void fraction with an MRE of less than 1.3% that is acceptable in the field of multi-phase flow-meters. However, this value of MRE is almost close to 1.4% that was obtained in our previous work [4], in which the void fraction was predicted independent of the flow regime using two detectors. An advantage of presented methodology is the use of just one detector which causes cost reduction of the measuring system.

References

[1] Abro, E., Johansen, G.A. (1999). Improved Void Fraction Determination by Means of Multibeam Gamma-Ray Attenuation Measurements. *Flow. Meas. Instrum.*, 10(2), 99–108.

[2] Roshani, G.H., Nazemi, E., Feghhi, S.A.H., Setayeshi, S. (2015). Flow regime identification and void fraction prediction in two-phase flows based on gamma ray attenuation. *Measurement.*, 62, 25–32.

[3] Adineh, M., Nematollahi, M., Erfaninia, A. (2015). Experimental and numerical void fraction measurement for modeled two-phase flow inside a vertical pipe. *Ann. Nucl. Energy.*, 83, 188–192.

[4] Nazemi, E., Roshani, G.H., Feghhi, S.A.H, Gholipour Peyvandi, R., Setayeshi, S. (2016). Precise Void Fraction Measurement in Two-Phase Flows Independent of the Flow Regime using gamma-ray attenuation. *Nucl. Eng. Technol.*, 48, 64–71.

[5] Roshani, G.H., Nazemi, E., Roshani, M.M. (2017). Identification of flow regime and estimation of volume fraction independent of liquid phase density in gas-liquid two-phase flow. *Prog. Nucl. Energ.*, 98, 29–37.

[6] El Abd, A. (2014). Intercomparison of gamma ray scattering and transmission techniques for gas volume fraction measurements in two phase pipe flow. *Nucl. Instrum. Meth. A.*, 735, 260–266.

[7] Roshani, G.H., Nazemi, E., Roshani, M.M. (2017). Usage of Two Transmitted Detectors with Optimized Orientation In order to Three Phase Flow Metering. *Measurement*, 100, 122–130.

[8] Hanus, R., Petryka, L., Zych, M. (2014). Velocity measurement of the liquid–solid flow in a vertical pipeline using gamma-ray absorption and weighted cross-correlation. *Flow. Meas. Instrum.*, 40, 58–63.

[9] Roshani, G.H., Nazemi, E., Roshani, M.M. (2017). Flow regime independent volume fraction estimation in three-phase flows using dual-energy broad beam technique and artificial neural network. *Neural. Comput. Appl.*, 28, 1265.

[10] Roshani, G.H., Feghhi, S.A.H., Mahmoudi-Aznaveh, A., Nazemi, E., Adineh-Vand, A. (2014). Precise volume fraction prediction in oil-water-gas multiphase flows by means of gamma-ray attenuation and artificial neural networks using one detector. *Measurement.*, 51, 34–41.

[11] Mosorov, V., Zych, M., Hanus, R., Petryka, L. (2016). Modelling of dynamic experiments in MCNP5 environment. *Appl. Radiat. Isotopes.*, 112, 136–140.

[12] Roshani, G.H., Hanus, R., Khazaei, A., Zych, M., Nazemi, E., Mosorov, V. (2018). Density and velocity determination for single-phase flow based on radiotracer technique and neural networks. *Flow. Meas. Instrum.*, 61, 9–14.

[13] Hanus, L., Zych, M., R., Petryka, Swisulski, D. (2014). Time delay estimation in two-phase flow investigation using the γ-ray attenuation technique. *Math. Probl. Eng.*, 2014, 1–10.

[14] Roshani, G.H., Nazemi, E. (2017). A high performance gas–liquid two-phase flow meter based on gamma-ray attenuation and scattering. *Nucl. Sci. Tech.*, 28(11), 169.

[15] Nazemi, E., Roshani, G.H., Feghhi, S.A.H, Setayeshi, S., Gholipour Peyvandi, R. (2015). A radiation-based hydrocarbon two-phase flow meter for estimating of phase fraction independent of liquid phase density in stratified regime. *Flow. Meas. Instrum.*, 46, 25–32.

www.czasopisma.pan.pl PAN www.journals.pan.pl

G.H. Roshani, E. Nazemi, et al.: DESIGNING A SIMPLE RADIOMETRIC SYSTEM TO PREDICT . . .

[16] Nazemi, E., Roshani, G.H., Feghhi, S.A.H, Setayeshi, S., Eftekhari Zadeh, E., Fatehi, A. (2016). Optimization of a method for identifying the flow regime and measuring void fraction in a broad beam gamma-ray attenuation technique. *Int. J. Hydrogen. Energ.*, 41, 7438–444.

[17] Roshani, G.H., Nazemi, E., Roshani, M.M. (2017). Application of radial basis function in densitometry of stratified regime of liquid-gas two phase flows. *Radiat. Meas.*, 100, 9–17.

[18] Zych, M., Petryka, L., Kępiński, J., Hanus, R., Bujak, T., Puskarczyk, E. (2014). Radioisotope investigations of compound two-phase flows in an open channel. *Flow. Meas. Instrum.*, 35, 11–15.

[19] Salgado, C.M., Pereira, C.M.N.A., Schirru, R., Brandao, L.E.B. (2010). Flow regime identification and volume fraction prediction in multiphase flows by means of gamma-ray attenuation and artificial neural networks. *Prog. Nucl. Energ.*, 52, 555–562.

[20] Yadollahi, A., Nazemi, E., Zolfaghari, A., Ajorloo, A.M. (2016). Application of artificial neural network for predicting the optimal mixture of radiation shielding concrete. *Prog. Nucl. Energ.*, 89, 69–77.

[21] Karami, A., Roshani, G.H., Salehizadeh, A., Nazemi, E. (2017). The Fuzzy Logic Application in Volume Fractions Prediction of the Annular Three-Phase Flows. *J. Nondestruct. Eval.*, 36, 35.

[22] Hanus, R. (2015). Application of the Hilbert Transform to measurements of liquid-gas flow using gamma ray densitometry. *Int. J. Multiphas. Flow.*, 72, 210–217.

[23] Yadollahi, A., Nazemi, E., Zolfaghari, A., Ajorloo, A.M. (2016). Optimization of thermal neutron shield concrete mixture using artificial neural network. *Nucl. Eng. Des.*, 305, 146–155.

[24] Roshani, G.H., Nazemi, E., Roshani, M.M. (2017). A novel method for flow pattern identification in unstable operational conditions using gamma ray and radial basis function. *Appl. Radiat. Isotopes.*, 123, 60–68.

[25] Roshani, G.H., Nazemi, E., Roshani, M.M. (2017). Intelligent recognition of gas-oil-water three-phase flow regime and determination of volume fraction using Radial Basis Function. *Flow. Meas. Instrum.*, 54, 39–45.

[26] Roshani, G.H., Karami, A., Salehizadeh, A., Nazemi, E. (2017). The capability of radial basis function to forecast the volume fractions of the annular three-phase flow of gas-oil-water. *Appl. Radiat. Isotopes.*, 129, 156–62.

[27] Eftekharizadeh, E., Sadighzadeh, A., Salehizadeh, A., Nazemi, E., Roshani, G.H. (2016). Neutron activation analysis for cement elements using an IECF device as a high energy neutron source. *Analytical. Methods.*, 8(11), 2510–2514.

[28] Roshani, G.H., Nazemi, E., Feghhi, S.A.H. (2016). Investigation of using 60Co source and one detector for determining the flow regime and void fraction in gas-liquid two-phase flows. *Flow. Meas. Instrum.*, 50, 73–79.

[29] Pelowitz, D.B. (2005). MCNP-X TM User's Manual, Version 2.5.0. LA-CP-05e0369. Los Alamos National Laboratory.

[30] Amid, S., Mesri Gundoshmian, T. (2017). Prediction of output energies for broiler production using linear regression, ANN (MLP, RBF), and ANFIS models. *Environ. Prog. Sustain.*, 36(2), 577–585.

[31] Rakhshkhorshid, M. (2017). A Robust RBF-ANN Model to Predict the Hot Deformation Flow Curves of API X65 Pipeline Steel. *Iranian Journal of Materials Forming*, 4(1), 12–20.

[32] Niroomand-Toomaj, E., Etemadi, A., Shokrollahi, A. (2017). Radial basis function modeling approach to prognosticate the interfacial tension CO 2/Aquifer Brine. *J. MO.L LIQ.*, 238, 540–544.

[33] Wang, L., Liu, J., Yan, Y., Wang, X., Wang, T. (2017). Gas-Liquid Two-Phase Flow Measurement Using Coriolis Flowmeters Incorporating Artificial Neural Network, Support Vector Machine, and Genetic Programming Algorithms. *IEEE. T. Instrum. Meas.*, 66(5), 852–868.